Catalysis Science & Technology

PAPER

View Article Online
View Journal | View Issue

Cite this: *Catal. Sci. Technol.*, 2016, **6**, 4577

Direct C–H bond activation of ethers and successive C–C bond formation with benzene by a bifunctional palladium–titania photocatalyst†

Akanksha Tyagi,[a] Tomoya Matsumoto,[a] Tatsuhisa Kato[ab] and Hisao Yoshida*[ac]

Received 30th December 2015,
Accepted 9th February 2016

DOI: 10.1039/c5cy02290h

www.rsc.org/catalysis

Palladium-loaded titanium oxide was found to work as a bifunctional photocatalyst for functionalization of benzene with ether upon photoirradiation, without using any special reagents. The metal-loaded TiO_2 photocatalyst activated a C–H bond of ethers and the heterogeneous Pd metal nanoparticle catalyst promoted the successive C–C bond formation between benzene and the radical species. In this reaction, benzene reacted very selectively with the α-carbon of various ethers at least in the initial stage of the reaction. Kinetic and ESR studies revealed a detailed mechanism for the reaction.

1. Introduction

Activation of sp^3 C–H bonds is one of the most desired reactions in current chemistry because it provides an opportunity to utilize and convert abundant and inexpensive alkanes to valuable products.[1] Especially in the view of green and sustainable chemistry, the direct activation of these bonds promises efficient synthetic practices because the desired compounds can be prepared in a single step instead of the currently used multistep processes consuming extra reagents. However, this is not an easy reaction since these bonds have very low reactivity due to their high bond strength and attainment of electronic saturation.[2]

Some of the earliest methods for sp^3 C–H bond activation have included the usage of strong acids or bases, but the harsh reaction conditions would limit the substrates available for the reaction. Since then, among notable advancements in this area, employing metal catalysts has become the most popular method, where the key idea is the formation of a new bond between the metal and the sp^3 carbon.[2] Even though these methods show higher efficiency and selectivity over the earlier methods, they all have inherent limitations. One is the sensitive nature of the involved reagents, *i.e.*, the preparation, storage and usage of these metal complexes should require air- or moisture-free conditions, which limits the applicability of these methods. The other is that some kinds of harmful and reactive reagents are often required. Hence, an innovative methodology for general and mild activation of sp^3 C–H bonds has been desired to be established.

In this regard, heterogeneous photocatalysis is a promising alternative.[3] In addition to the obvious advantages like simple product separation and reusability of heterogeneous catalysts, the use of photoenergy as the driving force would enable us to realize unique synthetic routes. Since the photoexcited electrons and holes themselves are very reactive, they can simultaneously but independently induce the reductive and oxidative reactions, respectively, thereby eliminating the use of other harmful and reactive chemicals. Thus, the reactions can be performed under mild conditions, making the process green and sustainable.

In our previous studies, we found that metal-loaded TiO_2 photocatalysts (M/TiO_2, M = Pd or Pt) can activate various types of chemicals to radical species under UV light. Based on this concept, we have reported the photocatalytic hydroxylation[4] and amination[5] of aromatic rings as well as the hydration of alkenes,[6] where we realized the activation of an O–H bond in water and an N–H bond in ammonia for the formation of rather difficult O–C and N–C bonds, respectively. It was considered that this strategy should be applicable to the activation of sp^3 C–H bonds in a similar way. To facilitate the reaction, we focused on molecules consisting of a functional group adjacent to the target sp^3 carbon, which would result in a decrease of the bond dissociation energy. For example, the bond dissociation enthalpy of a C–H bond in methane is *ca.* 426.8 kJ mol^{-1} while it becomes 401.6 kJ mol^{-1} in acetonitrile due to the adjacent cyano group.[7] This methodology has been firstly demonstrated in our previous study for the direct cyanomethylation of the benzene ring over Pd/TiO_2

[a] *Graduate School of Human and Environmental Studies, Kyoto University, Yoshida Nihonmatsu-cho, Sakyo-ku, Kyoto 606-8501, Japan. E-mail: yoshida.hisao.2a@kyoto-u.ac.jp*
[b] *Institute for Liberal Arts and Sciences, Kyoto University, Yoshida Nihonmatsu-cho, Sakyo-ku, Kyoto 606-8501, Japan*
[c] *Elements Strategy Initiative for Catalysts and Batteries (ESICB), Kyoto University, Kyotodaigaku-Katsura, Nishikyo-ku, Kyoto 615-8520, Japan*

† Electronic supplementary information (ESI) available: Effect of TiO_2 structure on the photocatalytic activity, catalytic reaction test in a flow reactor, ESR study, thermal effects on catalysis and adsorption and XAFS analysis of a Pd/TiO_2 sample. See DOI: 10.1039/c5cy02290h

photocatalysts,[8] where the adjacent cyano group would assist the C–H bond dissociation and stabilize the generated cyanomethyl radical to enhance the reaction efficiency for the successive C–C bond formation with benzene.

To expand this concept, ethers were examined in the present study, which were expected to become α-oxyalkyl radicals to realize the successive C–C bond formation for functionalization of benzene. We found for the first time that a bifunctional Pd/TiO_2 photocatalyst could successfully promote the direct sp^3 C–H bond activation in different ethers and the successive sp^3 C–sp^2 C bond formation with benzene to give ether-substituted benzenes (α-arylated ethers), an important class of compounds,[9] with almost complete selectivity and high yields. The yields obtained here are notable since these kinds of photocatalytic organic transformations have been crippled by low yields unless auxiliary chemicals or long reaction times are used.[4–6,8,10]

2. Experimental

2.1. Catalyst preparation

Various TiO_2 powder samples employed for the experiments were donated by the Catalysis Society of Japan as JRC-TiO-8 (anatase phase, 338 $m^2\ g^{-1}$), JRC-TiO-6 (rutile phase, 100 $m^2\ g^{-1}$) and JRC-TiO-4 (mixture of rutile and anatase phases, 50 $m^2\ g^{-1}$). All metal-loaded TiO_2 catalysts were prepared by the photodeposition method using the desired TiO_2 powder and an appropriate metal precursor solution of $PdCl_2$ (Kishida, 99%), $H_2PtCl_6{\cdot}6H_2O$ (Wako, 99.9%), $RhCl_3{\cdot}3H_2O$ (Kishida, 99%) or $HAuCl_4{\cdot}4H_2O$ (Kishida, 99.9%). The TiO_2 powder (4 g) was dispersed in ion-exchanged water (300 ml) and was irradiated with a ceramic xenon lamp (PE300 BUV) for 30 min. Then, methanol (100 ml) and the desired amount of the metal precursor solution were added to the suspension and the contents were stirred for 15 min without irradiation, followed by 1 h of stirring under light. It was then filtered off with suction, washed with ion-exchanged water and dried at 323 K for 12 h so as to obtain the metal-loaded TiO_2 photocatalysts. The catalysts were referred to as M(x)/TiO_2, where M indicates Pd, Pt, Rh or Au, and x indicates the loading amount of the metal species in weight%.

2.2. Catalyst characterization

Pd K-edge XAFS (X-ray absorption fine structure) analysis was carried out to determine the state of metal nanoparticles loaded over TiO_2 after the reaction. The spectra were recorded at NW10A of Photon Factory at the Institute of Materials Structure Science, High Energy Accelerator Research Organization (KEK-PF, Tsukuba, Japan) with a Si(311) double-crystal monochromator at room temperature. For the prepared catalyst samples, the spectra were recorded in the fluorescence mode by using a Lytle detector filled with a krypton (100%) flow equipped with a Ru filter ($\mu t = 6$) for the fluorescence and an ion chamber filled with an argon (100%) flow for the incident X-ray. The spectra of the reference samples were measured in the transmission mode. The spectra were analysed with REX 2000 software (Rigaku).

2.3. Reaction test

2.3.1. Materials. All chemicals were of analytical grade and used without further purification. The amounts of products were determined from the GC-MS calibration curve of the authentic samples procured from the industries.

2.3.2. Procedure for reaction tests. Before a photocatalytic reaction test, the M(x)/TiO_2 sample (0.1 g) in a Pyrex glass tube (70 mL) was subjected to pre-treatment for 1 h under the xenon lamp light of more than 350 nm wavelength using a long pass filter so as to clean its surface. Then, the reaction chamber was purged with argon gas for 10 minutes followed by the addition of reactants, benzene and ether, and stirring under light for the desired reaction time at room temperature. After irradiation, a portion of the gaseous phase was collected by means of an air-tight syringe and was analyzed using a GC-TCD (Shimadzu, GC-8A). Then, the reaction mixture was diluted with ethanol, followed by sampling of the liquid phase using a syringe attached with a PTFE filter to separate the M(x)/TiO_2 sample, and then analysed using a GC-MS (Shimadzu, GCMS-QP5050A).

The durability and reusability of the M(x)/TiO_2 sample was determined using a flow reactor, the details of which are explained in the ESI.†

2.3.3. Mechanistic studies. An ESR study was carried out in order to validate the formation of radical species from ether in the presence of UV light and the M(x)/TiO_2 samples. ESR measurements were performed at room temperature with an X-band spectrometer (JEOL-RE2X) by using JEOL's TE_{011} cavity for the samples. PBN (*N-tert*-butyl-α-phenylnitrone) was chosen as the spin trapping agent. For the ESR experiments, a suspension consisting of PBN (0.09 g), diethyl ether (DEE, 1 ml) and the Pd(0.1)/TiO_2 catalyst (0.02 g) was prepared and a portion of this suspension was then introduced into the ESR cavity. The contents were then irradiated using the light of >400 nm wavelength through a long-pass filter from a xenon lamp for about 20 min with simultaneous ESR measurement at room temperature. Additional information is shown in the ESI.†

Further information about the mechanism was obtained from the results of reaction tests using isotopic compounds such as deuterated diethyl ether, $(C_2D_5)_2O$, and deuterated benzene, C_6D_6, and temperature-controlled reaction tests.

3. Results and discussion

3.1. Catalytic reaction between benzene and diethyl ether over M(x)/TiO_2 samples

The reaction between benzene and diethyl ether (DEE, **1a**) with a Pd(0.2)/TiO_2 sample gave 1-ethoxyethylbenzene (1-EEB, **2a**) as the major product through the sp^2 C–sp^3 C bond formation between benzene and the α-position of DEE (Table 1, entry 1), while a trace amount of 2-ethoxyethylbenzene (2-EEB), a product of the reaction with the β-position of DEE, was also obtained (not shown). The benzene conversion to

Table 1 Results of the reaction tests between different benzenes and ethers with a Pd(0.2)/TiO_2 bifunctional photocatalyst

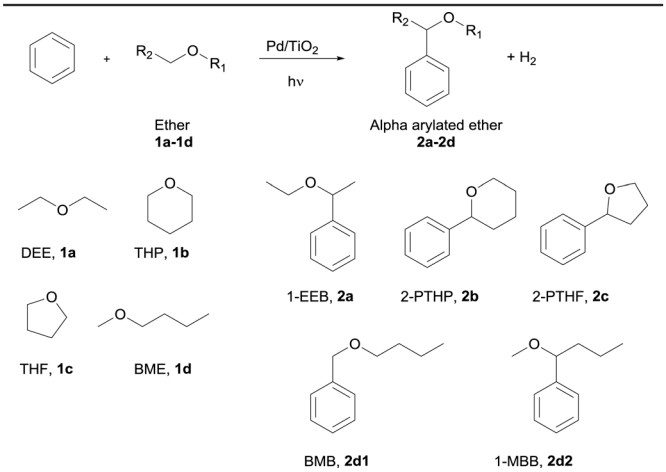

Entry	Ether	Product	Reaction time (h)	Amount of product[a] (μmol)	Y[b] (%)	S[c] (%)
1[d]	**1a**	**2a**	3	12.9	23	99
2[e]	**1b**	**2b**	3	16.8	30	99
3[f]	**1c**	**2c**	3	4.1	18	99
4[g]	**1d**	**2d1**	1	4.1	1.1	99
		2d2		7.9		

[a] GC-MS yield. [b] Y (%): yield of the listed product = 100 × (the amount of the product)/(the initial amount of benzene). [c] S (%): selectivity for the listed product among the benzene-containing products = 100 × (amount of the product)/(total amount of benzene-containing products). [d] 0.1 g of the Pd(0.2)/TiO_2 sample was used; the wavelength of incident light was ≥350 nm; the light intensity was 56 mW cm^{-2} when measured at 365 ± 20 nm wavelength using a UV radiometer (Topcon, UVR-2, UD-36); 5 μl (56 μmol) of benzene, 2 ml (19.2 mmol) of DEE and 0.4 μl of water were used; 1-EEB: 1-ethoxyethylbenzene; the amount of 1-EEB was determined from the calibration curve of 1-EEB. [e] 5 μl (56 μmol) of benzene, 2 ml (20 mmol) of THP and 0.4 μl of water were used; other conditions were the same as those mentioned above; 2-PTHP: 2-phenyltetrahydropyran; the amount of 2-PTHP was tentatively determined from the calibration curve of 1-methoxybutylbenzene (1-MBB). [f] 2 μl (22 μmol) of benzene, 1 ml (12 mmol) of THF and 0.4 μl of water were used; the remaining conditions were the same as those mentioned above; 2-PTHF: 2-phenyltetrahydrofuran; the amount of 2-PTHF was tentatively determined from the calibration curve of 1-EEB. [g] 100 μl (1.12 mmol) of benzene, 0.35 ml (1.19 mmol) of BME and 4 μl of water were used; the remaining conditions were the same as those before; BMB: butoxymethylbenzene, 1-MBB: 1-methoxybutylbenzene; the amounts of 1-MBB and BMB were determined from the calibration curve of 1-MBB.

the main product, 1-EEB, reached 23% for the initial 3 h. Caronna *et al.*[11] reported the C–C bond formation between a reactive heteroarene and ether over a TiO_2 photocatalyst with the aid of H_2O_2 as an additional radical generator. In contrast, our system employing the Pd/TiO_2 sample was free from such an auxiliary reagent and could work under much milder conditions to give the desired products with complete selectivity and high yields.

The high selectivity for α-substitution can be attributed to the lower bond dissociation enthalpy of the α-C–H bonds (397.4 kJ mol^{-1} for DEE) compared to their β-counterparts (426.8 kJ mol^{-1} for DEE).[12] Although some homocoupling products of DEE such as 2,3-diethoxybutane and its derivatives were also formed, the quantity was small. This means that the generated α-oxyalkyl radical would preferentially react with benzene before reacting with DEE or another α-oxyalkyl radical under these conditions. It is important to note that biphenyl, the dimer of the phenyl radical, was not detected at all under the examined reaction conditions. Among the gaseous products, hydrogen was the major product while very small amounts of methane and ethane were also detected.

Among the various M(*x*)/TiO_2 samples tested, the ones loaded with Pd, Pt or Rh were active while the Au(0.1)/TiO_2 sample was inactive for the C–C bond formation (Table 2, entries 1–4). Also, among the various TiO_2 tested for this reaction, with Pd as the co-catalyst, anatase phase TiO_2 (JRC-TiO-8) having a large specific surface area exhibited maximum activity (Table S1, ESI†). The selectivity for the α-arylated ether (1-EEB) was always high over these metal-loaded TiO_2 samples (more than 88% in Table 2 and Table S1†). The desired product was not formed in the absence of light (Table 2, entry 8) or the M(*x*)/TiO_2 sample (Table 2, entry 9), indicating that the reaction needed both light and the M(*x*)/TiO_2 sample. Moreover, when the reaction was performed with a pristine TiO_2 sample, only a very small amount of products was obtained (Table 2, entry 10), highlighting the importance of metal loading. It is notable that the Pd(*x*)/TiO_2 samples exhibited the highest activities for this reaction and the highest selectivity, more than 98%, for the α-arylated ether among the M(*x*)/TiO_2 samples (Table 2, entries 1, 5–7). For the Pd(0.1)/TiO_2 sample, the amount of 1-EEB was as high as 18.8 μmol (Table 1, entry 1) which corresponds to a TON (turnover number) of *ca.* 20 for 1 h per Pd atom in the system and this value further increased with time. These results

Table 2 Results of the reaction tests between benzene and DEE with various M(*x*)/TiO_2 samples[a]

Entry	Sample	Products[b] (μmol) 1-EEB	Products[b] (μmol) 2-EEB	$S_{1\text{-EEB}}$[c] (%)
1	Pd(0.1)/TiO_2	18.8	0.3	98
2	Pt(0.1)/TiO_2	1.8	0.2	90
3	Rh(0.1)/TiO_2	1.6	0.2	88
4	Au(0.1)/TiO_2	0	0	0
5	Pd(0.05)/TiO_2	10.8	0.2	98
6	Pd(0.2)/TiO_2	19.2	0.4	98
7	Pd(0.5)/TiO_2	12.8	0.1	99
8[d]	Pd(0.1)/TiO_2	0	0	0
9[e]	—	0	0	0
10[f]	TiO_2	0.6	0.1	86

[a] Reaction conditions: 3.3 ml (31.7 mmol) of DEE, 0.7 ml (7.8 mmol) of benzene and 0.1 g of the M(*x*)/TiO_2 sample were used, reaction time was 1 h, $\lambda \geq 350$ nm, and I = 40 mW cm^{-2} (at 365 ± 20 nm). [b] 1-EEB: see Table 1, 2-EEB: 2-ethoxyethylbenzene; the amount of 2-EEB was tentatively determined from the calibration curve of 1-EEB. [c] $S_{1\text{-EEB}}$ (%): selectivity for 1-EEB = 100 × (amount of 1-EEB)/(total amount of benzene-containing products). [d] No light was supplied during the reaction. [e] No photocatalyst was used and only light was supplied. [f] 0.1 g of pristine TiO_2 (anatase) was used for the reaction.

confirmed that this reaction should be a photoinduced catalytic reaction.

In fact, the amount of products did not increase drastically when the reaction time increased from those indicated in Table 1 to the longer one such as 5 h in these conditions. This might be due to the fact that the present reactor is a closed batch reactor which has some limitations. In a closed reactor, the reactants or the products including an undetectable amount of the by-products could be adsorbed on the catalyst surface which might cover the active sites and thus decrease the activity. Thus, the reaction seemed to stop after a certain period and no significant increase in product amount was observed. To support this proposal, the same reaction was also performed in a fixed-bed flow reactor as shown in the ESI.† The results evidenced that the photocatalyst had a long life as it maintained a constant activity for almost 10 h (Fig. S1†). This can be explained by considering the fact that, in a flow reactor, the reactants are being constantly removed from the catalyst bed which does not allows the attainment of adsorption–desorption equilibrium. Thus, the catalyst surface would be relatively uncovered in a flow reactor than a closed batch reactor. In fact, the catalyst was active enough to be reused for the next cycle without any pre-treatment (Fig. S2†).

3.2. Catalytic reaction between benzene and other ethers over the Pd(0.2)/TiO_2 sample

This reaction proceeded well with other ethers too (Table 1, entries 2–4). The reaction between benzene and THP (**1b**) gave 2-phenyltetrahydropyran (2-PTHP, **2b**) selectively, where the benzene conversion to the product reached 30% for the initial 3 h. THF (**1c**) also reacted with benzene selectively at the α-position to give 2-phenyltetrahydrofuran (2-PTHF, **2c**) with high benzene conversion (18%) for 3 h. BME (**1d**), with two α-carbons, gave two kinds of α-substituted products, butoxymethylbenzene (BMB, **2d1**) and 1-methoxybutylbenzene (1-MBB, **2d2**). In this case, the yield of the α-substituted products was not high and many by-products were observed, which could be because the α-oxymethylene radical formed from BME, which would produce BMB, would be less stable and preferentially converted to other compounds before reacting with benzene.

3.3. Mechanistic studies

3.3.1. ESR measurements. Referring to our previous studies[4–6,8,13] and considering the by-product formation, it could be proposed that the reaction would start with the photocatalytic radical formation from ether. Fig. 1 shows an ESR spectrum of the formed radical species from DEE in the presence of PBN as the spin trapping agent. The signals present between the Mn marker (Mn^{2+}), with the *g*-value of 2.0060, originate from the DEE–PBN spin adduct (eqn (S1)†). They represent a triple doublet originating from the nitrogen (triplet) of PBN with the hyperfine coupling constant of A_N = 1.39 mT and the hydrogen (doublet) at the α-carbon of PBN with A_H = 0.23 mT.

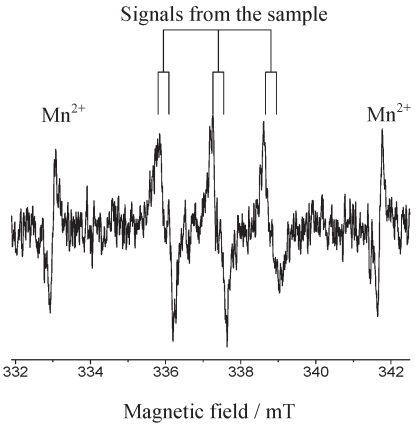

Fig. 1 ESR spectrum of the DEE radical with PBN as a spin trap.

These signals were different from those observed when the photodissociation of PBN took place under UV light (ESI†). Moreover, no signals were observed in the absence of DEE, the Pd/TiO_2 photocatalyst and light. Thus, it was confirmed that the reaction involves the oxidation of ether molecules to the radical species in the presence of the Pd(0.1)/TiO_2 photocatalyst under UV light irradiation (eqn (1)).

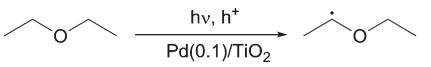

(1)

3.3.2. Study of kinetic isotope effect (inverse isotope effect). In order to get more insight about the mechanism of this reaction, isotope experiments were performed, and the results are shown in Table 3. For the reaction between deuterated benzene and DEE, the value of k_H/k_D was 0.92 (Table 3, entry 2) while that for the reaction between benzene and deuterated DEE was 0.93 (Table 3, entry 3). The values of k_H/k_D were not larger than unity for these reactions, which indicates that the C–H bond is not cleaved during the rate-determining step. Thus, surprisingly it can be concluded that the C–H bond activation of both benzene and DEE would not be the rate-determining step for this reaction.

However, it is important to consider the small inverse kinetic isotope effect (KIE) observed for each reaction. In order to give the α-arylated product, the reaction must involve the attack of the α-oxyalkyl radical on the benzene ring. This should involve a transition state where the hybridization of the benzene carbon would change from sp^2 to sp^3. This

Table 3 Results of isotope experiments for the reaction between benzene and DEE[a]

Entry	Reactants		Product, 1-EEB (μmol)	k_H/k_D[b]
1	Benzene	DEE	7.0	—
2	Benzene-d_6	DEE	7.6	0.92
3	Benzene	DEE-d_{10}	7.5	0.93

[a] Reaction conditions: 0.1 ml (1.1 mmol) of benzene, 0.4 ml (3.8 mmol) of DEE and 0.0125 g of the Pd(0.2)/TiO_2 catalyst were used, reaction time was 1 h, $\lambda \geq 350$ nm, and I = 40 mW cm^{-2} (at 365 ± 20 nm). [b] k_H/k_D was determined from the amounts of 1-EEB produced in entries 1 and 2 for entry 2 and those in entries 1 and 3 for entry 3.

change mainly effects the out-of-plane bending vibration of the C–H bond which is observed at 1350 cm^{-1} for the sp^3 C atom and 800 cm^{-1} for the sp^2 C atom.[14] Thus, when deuterated benzene was used, the change of the zero-point energies from sp^2 C to sp^3 C should be considered. Quantitatively, the difference in the zero-point energies for the C–H bonds in the reactants and the transition state is 550 cm^{-1} (800 cm^{-1} and 1350 cm^{-1}, respectively) while that for the C–D bonds is 403.2 cm^{-1} (586.8 cm^{-1} and 990 cm^{-1}, respectively). Thus, because the difference in the zero-point energies at the change from sp^2 to sp^3 for the C–D bonds is smaller than that for the C–H bonds, an inverse kinetic isotope effect should be observed. This could exactly explain what was observed for the reaction test between deuterated benzene and DEE (Table 3, entry 2). On the other hand, as for the inverse KIE observed for the reaction between benzene and deuterated DEE (Table 3, entry 3), other reasons should be considered. As discussed above, the attack of the DEE radical on benzene would generate a sp^3 like transition state. Since D atom is heavier than H atom, the C–D bond is stronger than the C–H bond. This causes the C–D bond to be slightly shorter than C–H bond. Thus, the transition state would be less sterically-crowded in the case of D than H, because of which the reaction of benzene with deuterated DEE will give an inverse KIE (Table 3, entry 3). Thus, from the above results, it can be concluded that the α-oxyalkyl radical would attack the carbon in the benzene molecule to form the reaction intermediate having the sp^3-like carbon centre in the aromatic ring (eqn (2)) and this step is most likely to be the rate-determining step for this reaction.

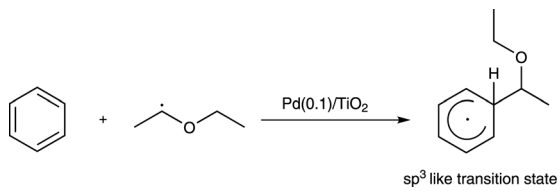

(2)

This neutral reaction intermediate would release a hydrogen radical to give the product (eqn (3)).

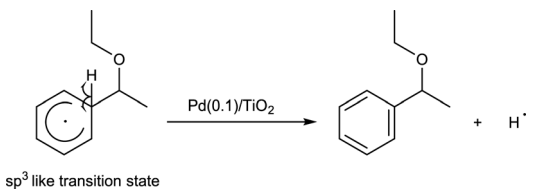

(3)

3.3.3. Study of temperature dependence. The reaction between the benzene molecule and the α-oxyalkyl radical to form the reaction intermediate (eqn (2)) would not be a photo-related process but a thermal process. This means that the whole reaction might be further promoted at higher temperature. If so, this might be the rate-determining step. In addition, it should be considered that other possible slow steps, such as adsorption of reactants or desorption of products, might also be candidates for the rate-determining steps and might be thermally accelerated. These possibilities were examined *via* the temperature-controlled reaction tests as described in the ESI.†

As a result, the amount of 1-EEB increased when the reaction was carried out at higher temperature under light (Table S2,† entries 1–4). However, no product was formed in the test at higher temperature in the dark (Table S2,† entry 5), eliminating the possibility that the thermal catalytic reaction with the Pd metal catalyst proceeds independently at higher temperatures. The apparent activation energy determined from the Arrhenius plot was 35.4 kJ mol^{-1} (Fig. 2a). It was further confirmed that the increase in the amount of 1-EEB at higher temperature was not due to its increased desorption from the catalyst surface in the adsorption–desorption equilibrium (Table S3†). The variation of the amount of desorbed 1-EEB with temperature gave a very gentle slope of 5.5 kJ mol^{-1} (Fig. 2b), which was much lower than the thermal activation energy during the reaction under light. Thus, the increase with temperature under light should be mainly due to thermocatalysis promoted further at higher temperatures. This result indicates that the rate-determining step would be this thermal reaction between benzene and the α-oxyalkyl radical originating from ether, which would be promoted by the Pd catalyst, in the form of metallic Pd nanoparticles, with the apparent thermal activation energy of 35.4 kJ mol^{-1} and hence would be accelerated at higher temperatures.

3.4. State of Pd nanoparticles over TiO_2

The Pd K-edge XAFS spectra revealed the state of the Pd catalyst on TiO_2. Fig. 3A shows the normalized XANES spectra of the Pd(0.2)/TiO_2 catalyst sample and references, *i.e.*, a metallic Pd foil and a PdO powder sample. The spectrum of the catalyst sample exhibited similar oscillation to metallic Pd at the higher energy region of more than 24.4 keV although the post-edge feature was not identical to that of the metallic Pd foil. Obviously, this was quite different from that of the PdO sample.

Fig. S3† shows the differential spectra of these XANES. The differential spectrum of the Pd(0.2)/TiO_2 catalyst sample exhibited a similar shape to that of the Pd metal and different from that of PdO. The absorption edge values were evaluated

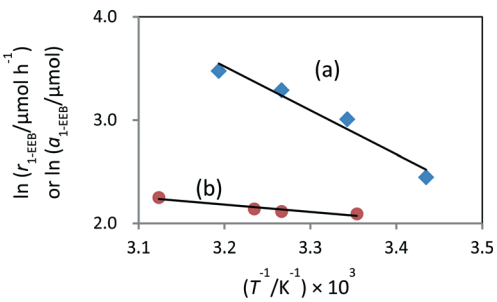

Fig. 2 Pseudo-Arrhenius plots for (a) temperature-controlled reactions between benzene and DEE under light and (b) adsorption tests of 1-EEB in the dark, with the Pd(0.2)/TiO_2 bifunctional photocatalyst. $r_{1\text{-EEB}}$: formation rate of 1-EEB; $a_{1\text{-EEB}}$: amount of desorbed 1-EEB in the solution.

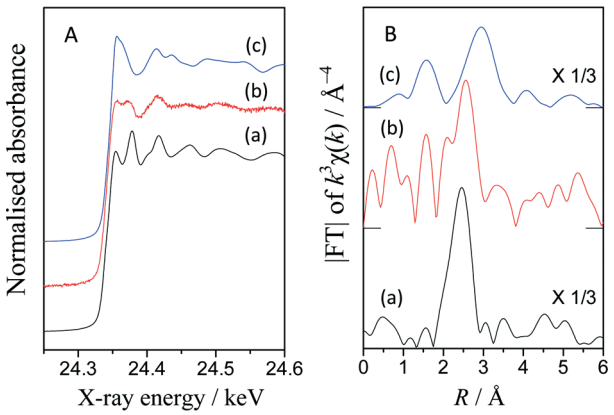

Fig. 3 Normalized XANES spectra (A) and Fourier transforms of the k^3-weighted EXAFS (B) of the metallic Pd foil (a), the Pd(0.2)/TiO_2 sample after the reaction test between benzene and DEE (b), and PdO powder (c). The intensity of the FT-EXAFS of the reference samples was reduced to one third.

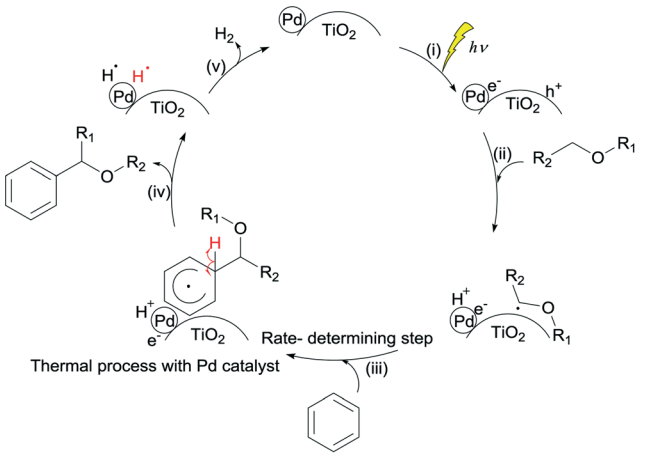

Fig. 4 Proposed mechanism of the reaction between benzene and ether by a bifunctional Pd/TiO_2 photocatalyst through the direct activation of the sp^3 C–H bond of ether to form the C–C bond with benzene.

from these spectra. Interestingly, the Pd(0.2)/TiO_2 catalyst sample showed a lower value (24.337 keV) than the Pd metal (24.346 keV) and PdO (24.349 keV), implying that the Pd species in the Pd(0.2)/TiO_2 catalyst might be electron-rich. It is known that, when TiO_2 and a precious metal nanoparticle form a semiconductor–metal junction, the electrons migrate to the metal particle, which would make the metal particle electron-rich. Thus, in the present case, the Pd nanoparticles loaded on the surface of TiO_2 might be negatively charged to some extent. In addition, during the reaction under photoirradiation, the photoexcited electron stored in the metallic Pd nanoparticle might further enhance this property.

Fig. 3B shows the Fourier-transformed EXAFS spectra. The peaks around 1.6, 2.5 and 3.0 Å correspond to the Pd–O shell in PdO, the Pd–Pd shell in the Pd metal and the Pd–Pd shell in PdO. Although the catalyst sample showed a noisy spectrum, the Pd–Pd shell in the Pd metal was clearly visible, indicating that the Pd species would be metallic. However, an additional peak was observed at 1.6 Å. According to the curve fitting analysis (Table S4†), the coordination number was 3.9 for the Pd–Pd shell and 1.5 for the Pd–O shell. This suggests that the Pd species on the TiO_2 surface would be metallic Pd nanoparticles connected to the TiO_2 surface through oxygen atoms.

Thus, it can be proposed that the Pd species in the Pd(0.2)/TiO_2 catalyst would be in the metallic state during the photocatalytic reaction between benzene and DEE. This further suggests that the Pd particles in the sample can function as an electron-rich metal catalyst during this reaction, making the catalyst a bifunctional photocatalyst. This electron-rich property might be advantageous to inducing electron donation to the anti-bonding π* molecular orbital of the adsorbed benzene to activate it.

3.5. Proposed mechanism

Based on these observations, it is clear that the Pd/TiO_2 catalyst can be recognised as a bifunctional catalyst comprising both the TiO_2 photocatalyst with the Pd co-catalyst and the Pd metal nanoparticle thermocatalyst. The reaction mechanism with the bifunctional catalyst can be proposed as follows.

The TiO_2 photocatalyst can be excited by photoirradiation to generate the excited electron (e^-) and hole (h^+) (Fig. 4, i). The hole would activate the α-C–H bond of ether to generate the α-oxyalkyl radical and a proton as shown in eqn (1) and (ii). Thereafter, the Pd nanoparticle would thermally catalyse the C–C bond formation between benzene and the α-oxyalkyl radical to form the reaction intermediate having the sp^3-like carbon centre in the aromatic ring (eqn (2) and (iii)). This step would be the rate-determining step under these conditions. The intermediate would release a hydrogen radical so as to give the desired alpha-substituted product (eqn (3) and (iv)). A proton would be reduced to a hydrogen radical by the photoexcited electrons present on the Pd surface which would couple with the previously eliminated hydrogen radical to form hydrogen (eqn (4) and (v)).

$$H^+ + e^- \xrightarrow{H^\cdot} H_2 \quad (4)$$

These reaction steps are summarised in the scheme shown in Fig. 4. It is proposed that this reaction should be a one-photon process.

4. Conclusions

In conclusion, we successfully achieved the direct activation of the sp^3 C–H bond in various ethers followed by their successive sp^3 C–sp^2 C bond formation with benzene by using a heterogeneous bifunctional catalyst that could function as both a photocatalyst and a palladium metal catalyst. The photocatalyst could activate the sp^3 C–H bond at the α-carbon in various ethers to form the α-oxyalkyl radical species and the palladium catalyst would promote the reaction between the aromatic ring of benzene and the radical species with the formation of the sp^3 C–sp^2 C bond to produce the ether-substituted benzene, *i.e.*, α-arylated ether.

We hope that this new strategy for direct C–H activation and successive C–C bond formation will be widely applicable to other reaction systems.

Acknowledgements

The XAFS experiments were performed under the approval of the Photon Factory Program Advisory Committee (Proposal No. 2014G547). This work was supported by JSPS KAKENHI Grant Number 25105723 for Scientific Research on Innovative Areas "Molecular Activation Directed towards Straightforward Synthesis".

Notes and references

1 R. G. Bergman, *Nature*, 2007, **446**, 391; K. Godula and D. Sames, *Science*, 2006, **312**, 67; *Handbook of C–H transformations*, ed. G. Diker, Wiley-VCH, Weinheim, Germany, 2005.

2 J. A. Labinger and J. E. Bercaw, *Nature*, 2002, **417**, 507; D. A. Colby, R. G. Bergman and J. A. Ellman, *Chem. Rev.*, 2009, **110**, 704; M. P. Doyle, R. Duffy, M. Ratnikov and L. Zhou, *Chem. Rev.*, 2010, **110**, 704.

3 M. Fagnoni, D. Dondi, D. Ravelli and A. Albini, *Chem. Rev.*, 2007, **107**, 2725; G. Palmisano, V. Augugliaro, M. Pagliaro and L. Palmisano, *Chem. Commun.*, 2007, 3425; Y. Shiraishi and T. Hirai, *J. Photochem. Photobiol., C*, 2008, **9**, 157; H. Yoshida, in *Environmentally benign photocatalysts: Applications of titanium oxide-based materials*, ed. M. Anpo and P. V. Kamat, Springer, 2010, ch. 27, p. 647; H. Kisch, *Angew. Chem., Int. Ed.*, 2013, **52**, 812.

4 H. Yoshida, H. Yuzawa, M. Aoki, K. Otake, H. Itoh and T. Hattori, *Chem. Commun.*, 2008, 4634; H. Yuzawa, M. Aoki, K. Otake, T. Hattori, H. Itoh and H. Yoshida, *J. Phys. Chem. C*, 2012, **116**, 25376.

5 H. Yuzawa and H. Yoshida, *Chem. Commun.*, 2010, **46**, 8854; H. Yuzawa, J. Kumagai and H. Yoshida, *J. Phys. Chem. C*, 2013, **117**, 11047.

6 H. Yuzawa, S. Yoneyama, A. Yamamoto, M. Aoki, K. Otake, H. Itoh and H. Yoshida, *Catal. Sci. Technol.*, 2013, **3**, 1739.

7 Y. R. Luo, *Handbook of Bond Dissociation Energies in Organic Compounds*, CRC Press, 2002; D. R. Lide, *CRC Handbook of Chemistry and Physics*, CRC Press, London, 86th edn, 2006.

8 H. Yoshida, Y. Fujimura, H. Yuzawa, J. Kumagai and T. Yoshida, *Chem. Commun.*, 2013, **49**, 3793.

9 P. G. M. Wuts and T. W. Greene, *Protective Groups in Organic Synthesis*, Wiley & Sons, New York, 4th edn, 2007, p. 102; P. P. Pradhan, J. M. Bobbitt and W. F. Bailey, *J. Org. Chem.*, 2009, **74**, 9524; Z. Song, J. Gong, M. Zhang and X. Wu, *Asian J. Org. Chem.*, 2012, **1**, 214; D. Lednicer, *Strategies for Organic Drug Synthesis and Design*, Wiley & Sons, Hoboken, 2008.

10 K. V. S. Rao, B. S. Srinivas, A. R. Prasad and M. Subrmahanyam, *Chem. Commun.*, 2000, 1533; S. Marinkovic and N. Hoffmann, *Chem. Commun.*, 2001, 1576.

11 T. Caronna, C. Gambarotti, L. Palmisano, C. Punta and F. Recupero, *J. Photochem. Photobiol., A*, 2005, **171**, 237.

12 F. Agapito, B. J. C. Cabral and J. A. M. Simoes, *J. Mol. Struct.: THEOCHEM*, 2005, **719**, 109.

13 H. Yuzawa and H. Yoshida, *Chem. Lett.*, 2013, **42**, 1336; H. Yuzawa and H. Yoshida, *Top. Catal.*, 2014, **57**, 984.

14 E. V. Anslyn and D. A. Dougherty, *Modern Physical Organic Chemistry*, ed. J. Murdzek, Edwards Brothers, 2005, ch. 8, p. 428.